Introduction

- Why Cepheids are important.
- Why *Resolving* a binary Cepheid is important.
- Why resolving a binary Cepheids from the ground is all but impossible.

What Follows

- A brief review of binaries in circular orbits.
- How to resolve a binary whose components have very different colors (Massa & Endal 1987, AJ, 93, 760).
- Application of the approach to two binary Cepheids.

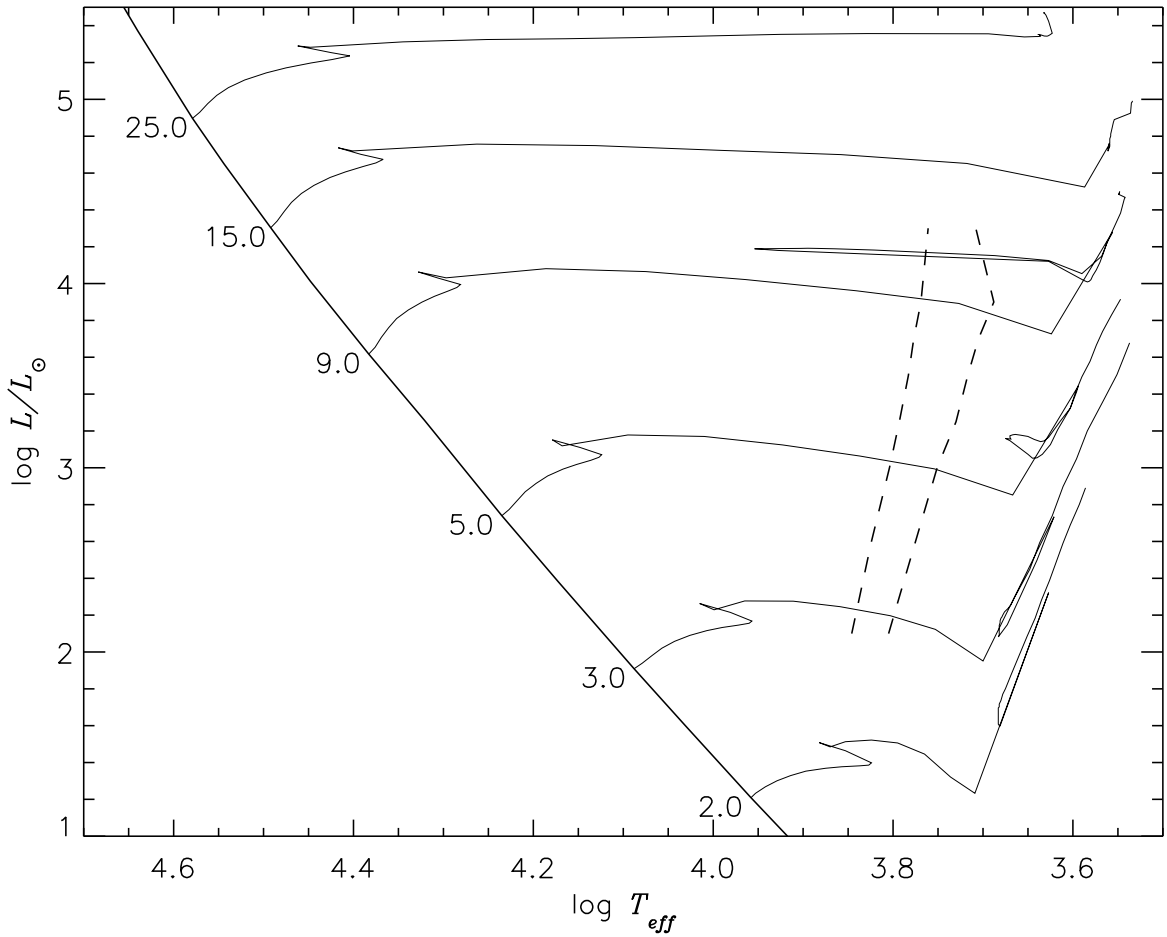

HRD showing the region occupied by the Cepheid variables. Notice that because the evolutionary tracks are nearly horizontal for these masses, a binary with a mass ratio near unity will consist of two components with nearly identical luminosities but *very* different temperatures.

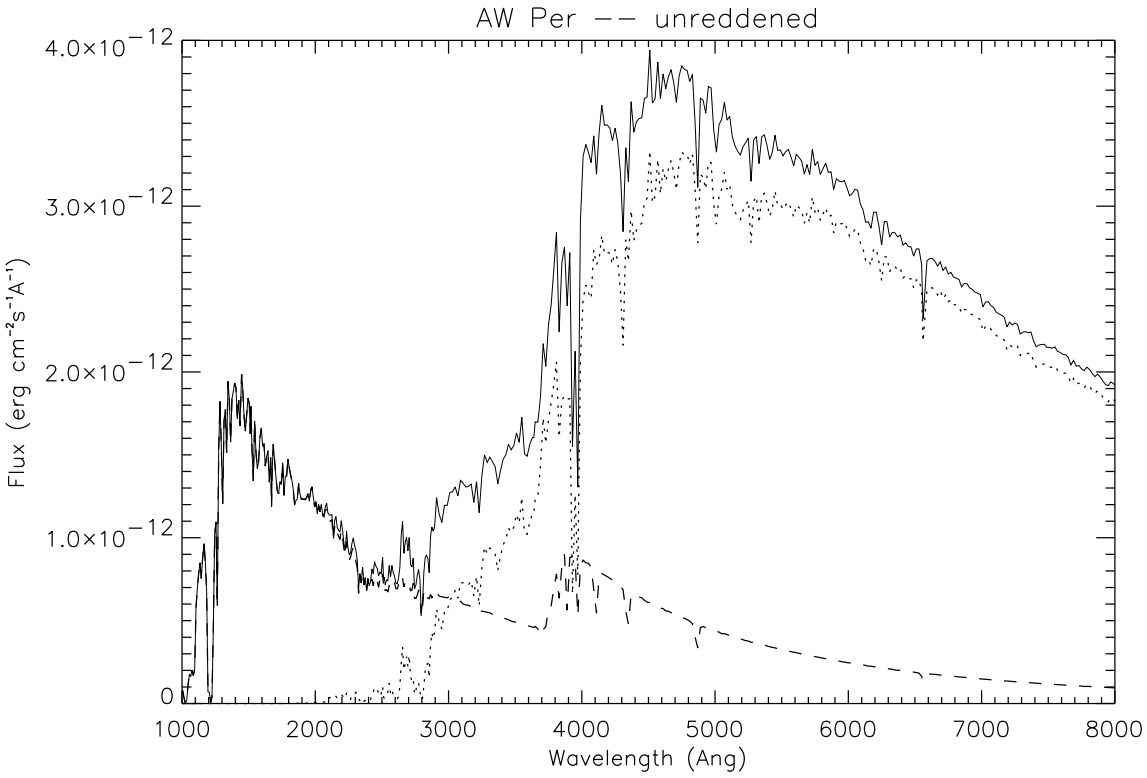

Model fluxes for AW Per (Evans 1994, ApJ, 363,273). The solid curve is the combined unreddened flux, the dotted curve is the contribution from the Cepheid primary, and the dashed curve is the contribution from the B-type secondary. Notice that the secondary is roughly 10 times fainter in the optical, making the system extremely difficult to resolve from the ground. On the other hand, the secondary dominates the flux from the system in the UV.

Basics for Binaries in Circular Orbits

Double lined spectroscopic binaries

Definition of center of mass:

$$r = r_1 + r_2 \tag{1}$$
$$r_1 M_1 = r_2 M_2 \tag{2}$$

Definition of period:

$$v_1 P = 2\pi r_1 \qquad v_2 P = 2\pi r_2 \tag{3}$$

Kepler's law:

$$P^2 = \frac{r^3}{M_1 + M_2} \tag{4}$$

Combining these gives

$$v_1 = \frac{2\pi M_2}{P^{1/3}(M_1 + M_2)^{2/3}}$$
$$v_2 = \frac{2\pi M_1}{P^{1/3}(M_1 + M_2)^{2/3}} \tag{5}$$

Therefore,

- If P, v_1 and v_2 are known, M_1 and M_2 can be found.
- With M_1 and M_2 known, r can be found.

Great, ***but***, only $v_1 \sin i$ and $v_2 \sin i$ are observed.

Getting $\sin i$ from the optical orbit

For a circle of radius a, tilted by $\sin i$ to the line of sight:

$$a^2 = x^2 + \frac{y^2}{\sin^2 i}$$

The separation as a function of θ on the sky is:

$$r = \frac{a \sin i}{\sqrt{\sin^2 i \cos^2 \theta + \sin^2 \theta}}$$

While the phase (θ in the plane of the circle) is:

$$\phi = \tan^{-1}\left(\frac{\tan \theta}{\sin i}\right)$$

Since

- ϕ is known from the spectrscopic orbit and
- r depends on only 2 variables, a and $\sin i$

Just two measurements of the optical orbit give a and $\sin i$ which give M_1, M_2 and d!

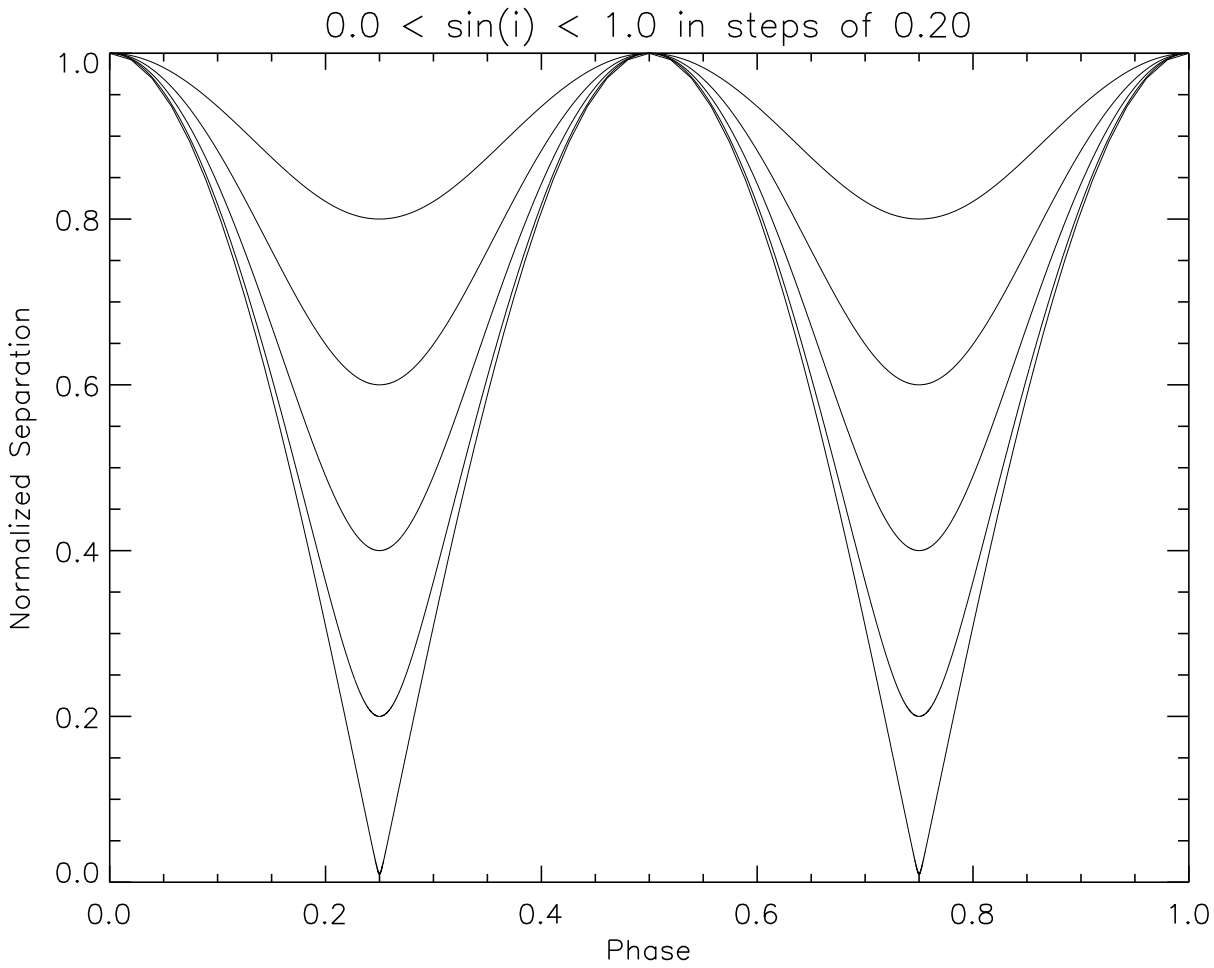

The normalized angular separation of a binary as a function of phase (period) for different values of $\sin i$. Notice that measurements at two, non-redundant phases determine the shape of the orbit and, hence, $\sin i$.

Angular Separations from Centroids

For a single star at $x = x_0$, let:

x = angular coordinate orthogonal to the dispersion
$h(x)$ = profile in the x direction
λ = coordinate parallel to the dispersion (wavelength)
$n(\lambda)$ = count rate at λ (counts s^{-1} $Å^{-1}$)
$N(\lambda)$ = total counts at λ (counts $Å^{-1}$)

The image of the spectrum is

$$I(\lambda, x) = N(\lambda)h(x - x_0)$$

For 2 stars centered at x_1 and x_2, let:

θ = the angular separation on the sky
ϕ = angle between north and a line connecting the stars
α = angle between north and the dispersion direction
$\Delta x \equiv x_2 - x_1$
$\Delta x = \theta \sin(\alpha - \phi)$
(when $\alpha - \phi = 0, \pm 180°, \Delta x = 0$)

The image of the binary spectrum is

$$I(\lambda, x) = N_1(\lambda)h(x - x_1) + N_2(\lambda)h(x - x_1 - \Delta x)$$

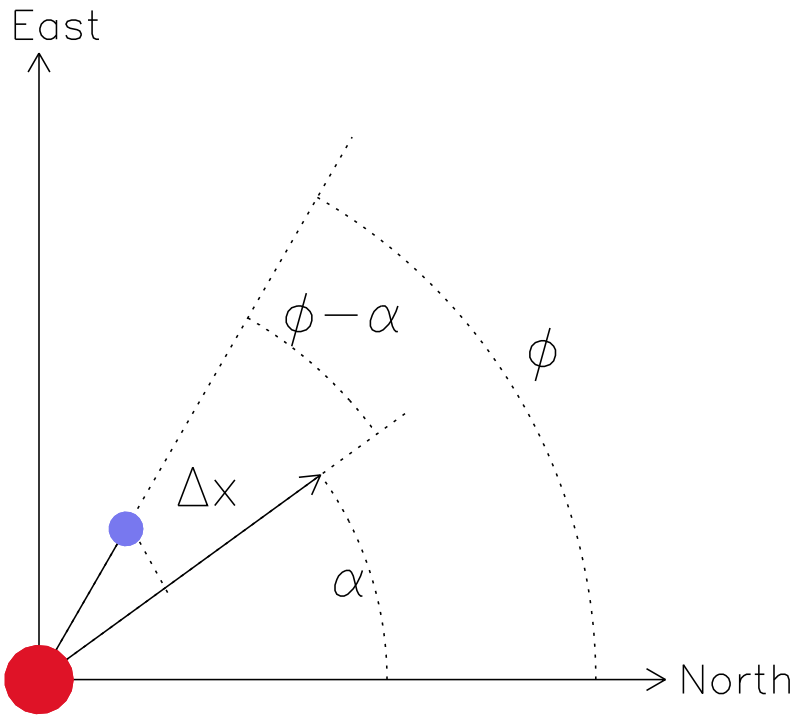

Diagram showing the definitions of the different angles used in the analysis, and their relations to one another.

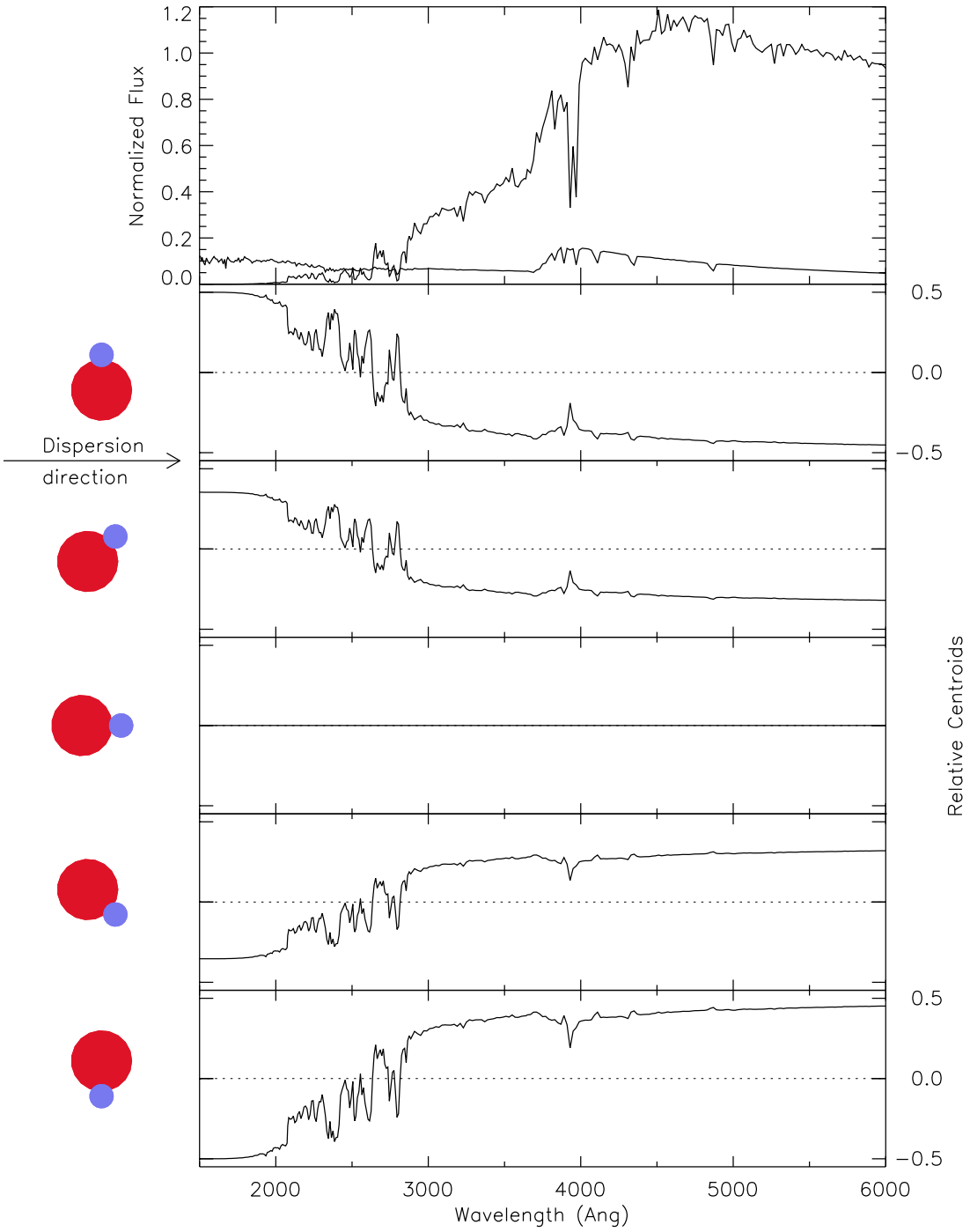

Kurucz models for a typical Cepheid (red) + B star (blue) binary. The top panel shows the relative fluxes of the components, and the next 5 panels show the wavelength dependence of the spectrum centroid for the orientations shown to the left of each panel. Notice how the wavelength dependence of the centroid changes with orientation and that the centroid shifts by less than 10% of the full separation in the optical. The "cross-over" point is not reached until $\lambda \sim 2500$Å.

If structure in $h(x)$ is $\ll \Delta x$

$$
\begin{aligned}
I(\lambda, x) &\simeq N_1(\lambda) h(x - x_1) + N_2(\lambda) \left[h(x - x_1) + \Delta x \frac{dh(x)}{dx}\bigg|_{x=x-x_1} \right] \\
&= [N_1(\lambda) + N_2(\lambda)] \left[h(x - x_1) + \frac{N_2(\lambda)}{N_1(\lambda) + N_2(\lambda)} \Delta x \frac{dh(x)}{dx}\bigg|_{x=x-x_1} \right] \\
&\simeq [N_1(\lambda) + N_2(\lambda)] h \left[\underbrace{x - \left(x_1 + \frac{\Delta x N_2(\lambda)}{N_1(\lambda) + N_2(\lambda)} \right)}_{Centroid} \right]
\end{aligned}
$$

Therefore, $x(\lambda)$ varies as

$$
\begin{aligned}
x(\lambda) &= x_1 + \frac{\Delta x N_2(\lambda)}{N_1(\lambda) + N_2(\lambda)} \\
&= x_1 + \frac{\Delta x}{1 + R(\lambda)}
\end{aligned}
$$

$$
x(\lambda) = x_1 + \Delta x [1 + R(\lambda)]^{-1}
$$

where $R(\lambda) \equiv N_1(\lambda)/N_2(\lambda)$ is the flux ratio of the components, and is determined from fitting the observed flux.

Extracting θ and ϕ from Δx

This requires observations at 2 or more α's

$$\begin{aligned} x(\lambda)^{(n)} &= x_1^{(n)} + \Delta x^{(n)}[1 + R(\lambda)]^{-1} \\ &= x_1^{(n)} + \theta \sin(\alpha^{(n)} - \phi)[1 + R(\lambda)]^{-1} \end{aligned}$$

where:

$x_1^{(n)}$ = *wavelength independent* position of star 1 in the n^{th} exposure (not known – entangled with placement errors)

$\alpha^{(n)}$ = α for the n^{th} observation

With $R(\lambda)$ known, regression of the $x(\lambda)^{(n)}$ on $R(\lambda)$ gives a set of $\Delta x^{(n)}$

Fitting the resulting $\Delta x^{(n)}$ to the function

$$\Delta x^{(n)} = \theta \sin(\alpha^{(n)} - \phi)$$

gives (ϕ, θ), the separation and position angle of the binary for the epoch of the observation.

Finally, two or more sets of observations at different epochs are required to determine $\sin i$ for the system.

Exposure Times and Errors

- Assume the PSF perpendicular to the dispersion is a Gaussian with $FWHM = \alpha$
- Then a single count is equivalent to one estimate of the center of the spectrum drawn from a sample with a $\sigma = 0.42\alpha$

Thus, for $n(\lambda)\Delta\lambda\Delta t$ samples (counts), the RMS uncertainty in the mean centroid over $\Delta\lambda$, $\langle x(\lambda)\rangle$, is

$$\sigma[\langle x(\lambda)\rangle] = \frac{0.42\alpha}{\sqrt{n(\lambda)\Delta\lambda\Delta t}}$$

The Observations

- Used *HST* to obtain optical to UV coverage.
- Used FOC for maximum spatial resolution and maximal wavelength coverage on a single detector.
- However, the FOC pixels are not true geometric entities.
- Obtained exposures at 3 roll angles 29° apart (to determine θ and ϕ).
- Obtained exposures at 3 different detector locations at each roll angle (to examine repeatability).

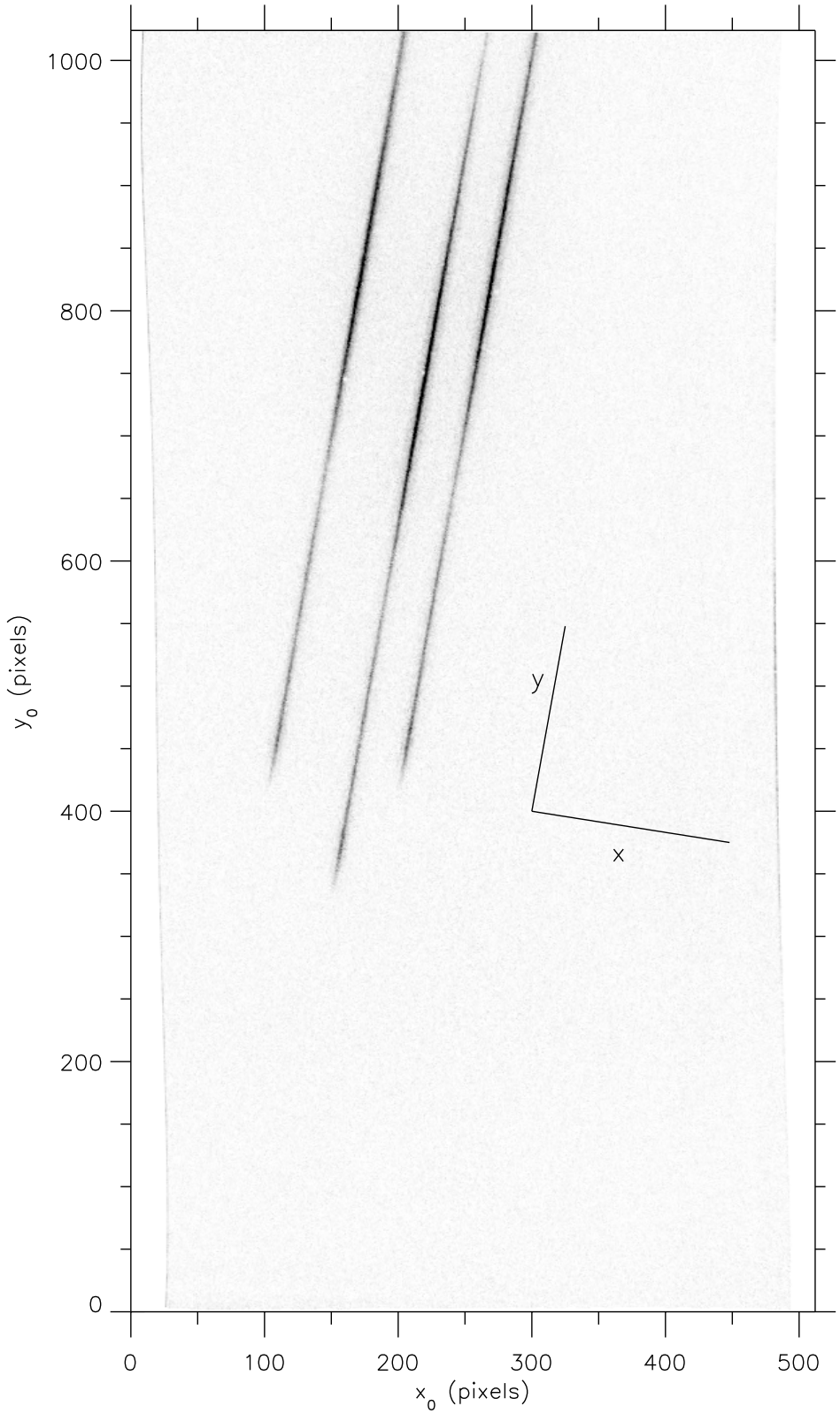

Superposition of three images of AW Per obtained at a single roll angle. This shows the effect of displacing the image for each sub-exposure, in order to determine the effects of localized distortions.

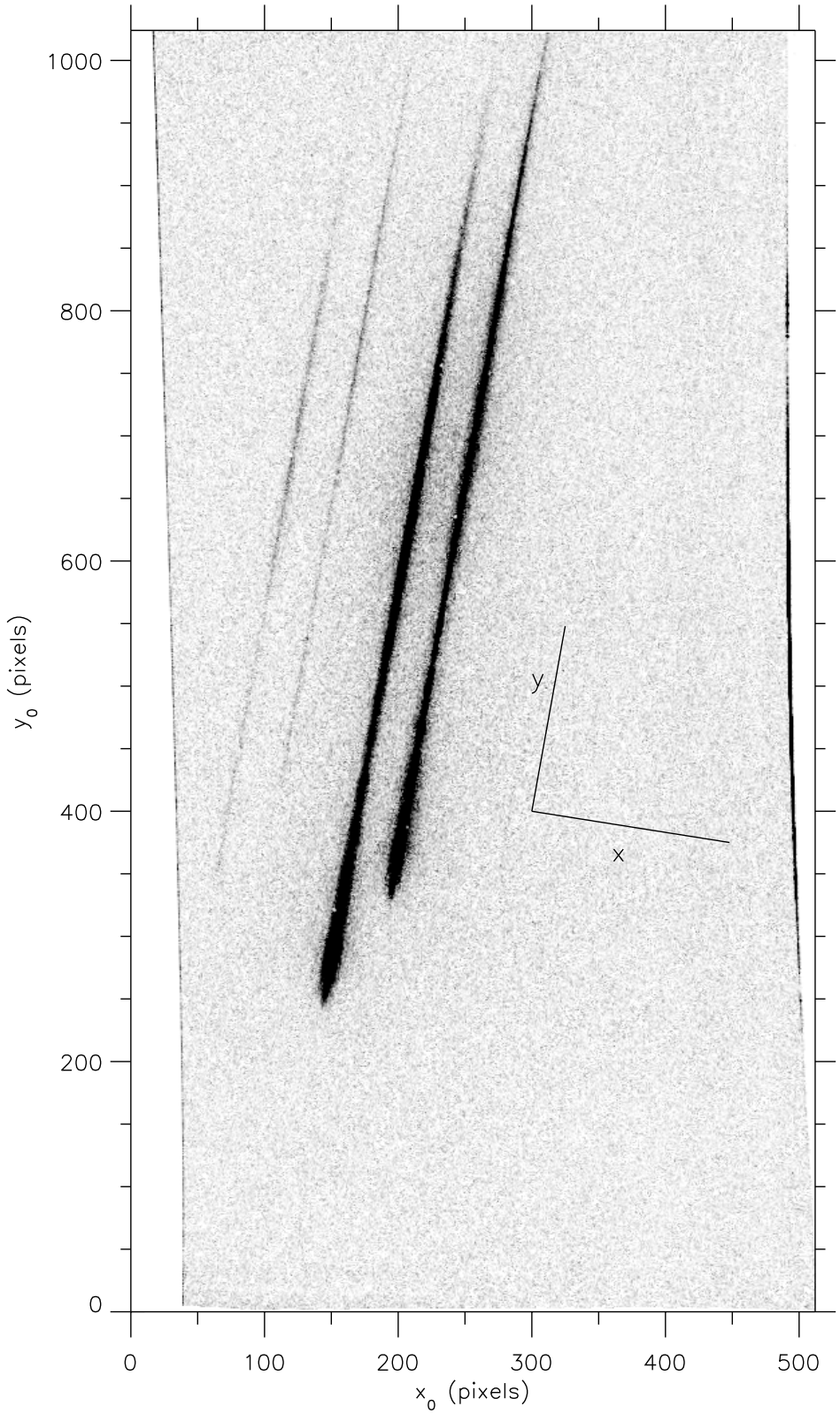

Superposition of two images of U Aql obtained at a single roll angle. This shows the effect of displacing the image for each sub-exposure, in order to determine the effects of localized distortions. The second, fainter spectrum in due to U Aql B.

Analysis

- Extracted $x(\lambda)$ via cross-correlation.
- Repeated observations at the same roll angle revealed residual low level geometric distortions.
- Used an FOC simulator and Kurucz models for $R(\lambda)$.
- Fit $R(\lambda)$ *and* a low order polynomial to the centroids to obtain $\Delta x^{(n)}$ at each roll angle.
- Found the θ and ϕ for the system by fitting the $\Delta x^{(n)}$ to $\theta \sin(\alpha^{(n)} - \phi)$.

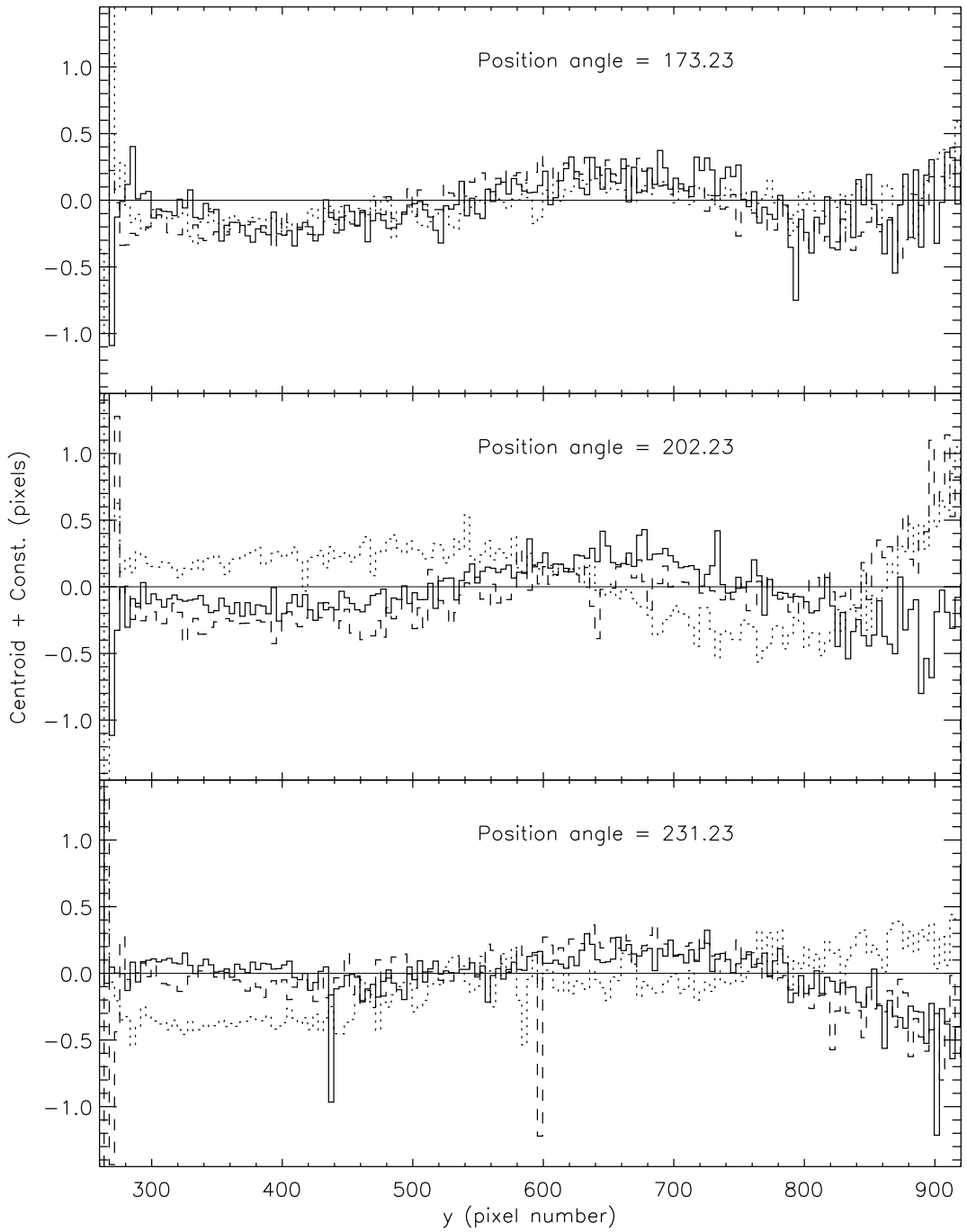

Superpositions of all the centroids obtained at each off-set for each roll (position) angle for U Aql. The scatters about the mean in each panel show the effects of localized, uncorrected distortions. Note, that the disagreement is smooth, and can be characterized by a low order polynomial.

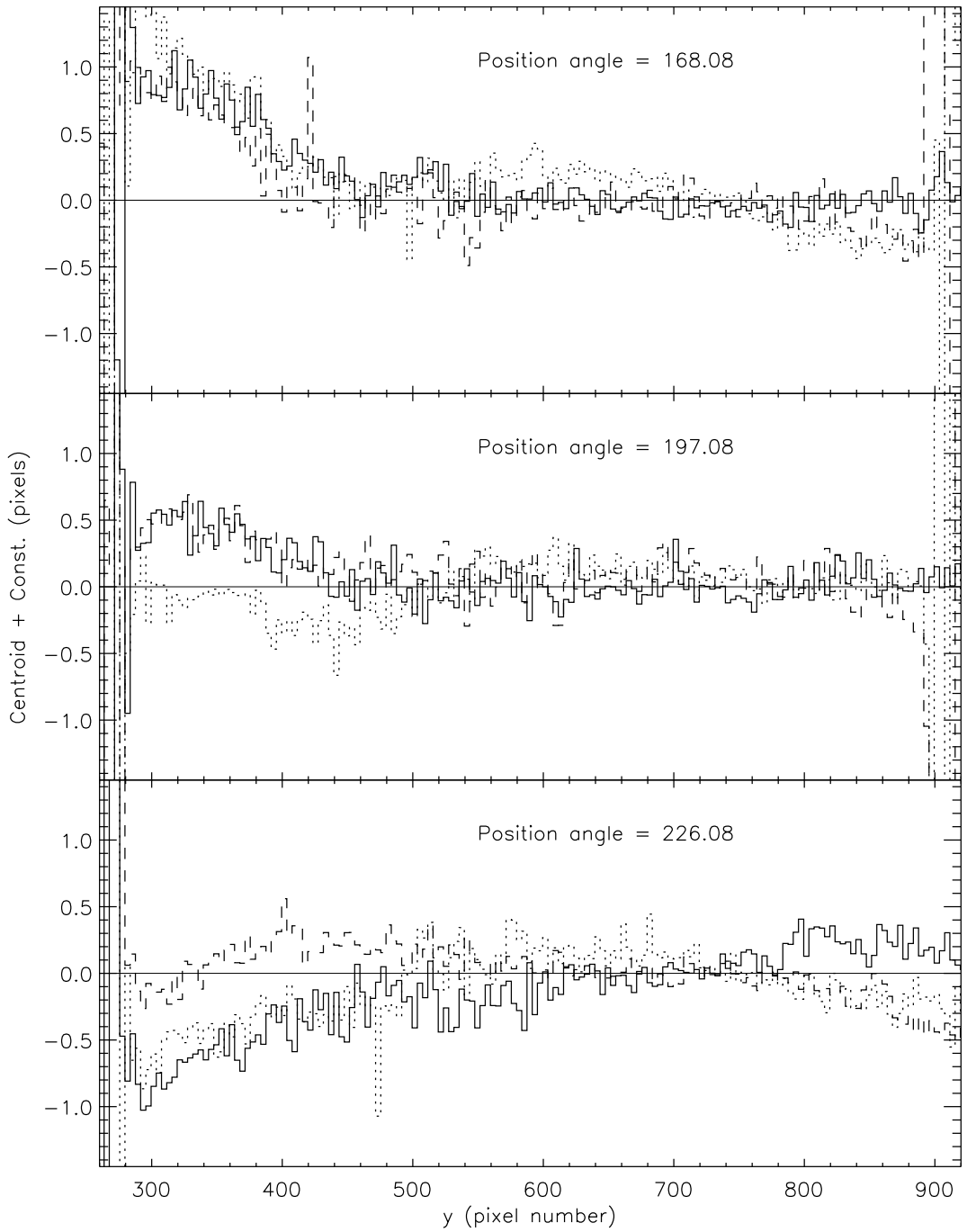

Superpositions of all the centroids obtained at each off-set for each roll (position) angle for AW Per. The scatters about the mean in each panel show the effects of localized, uncorrected distortions. Note, that the disagreement is smooth, and can be characterized by a low order polynomial. Notice that for a position angle of 168.08°, the centroids have a very distinctive shape, which is unlike a low order polynomial.

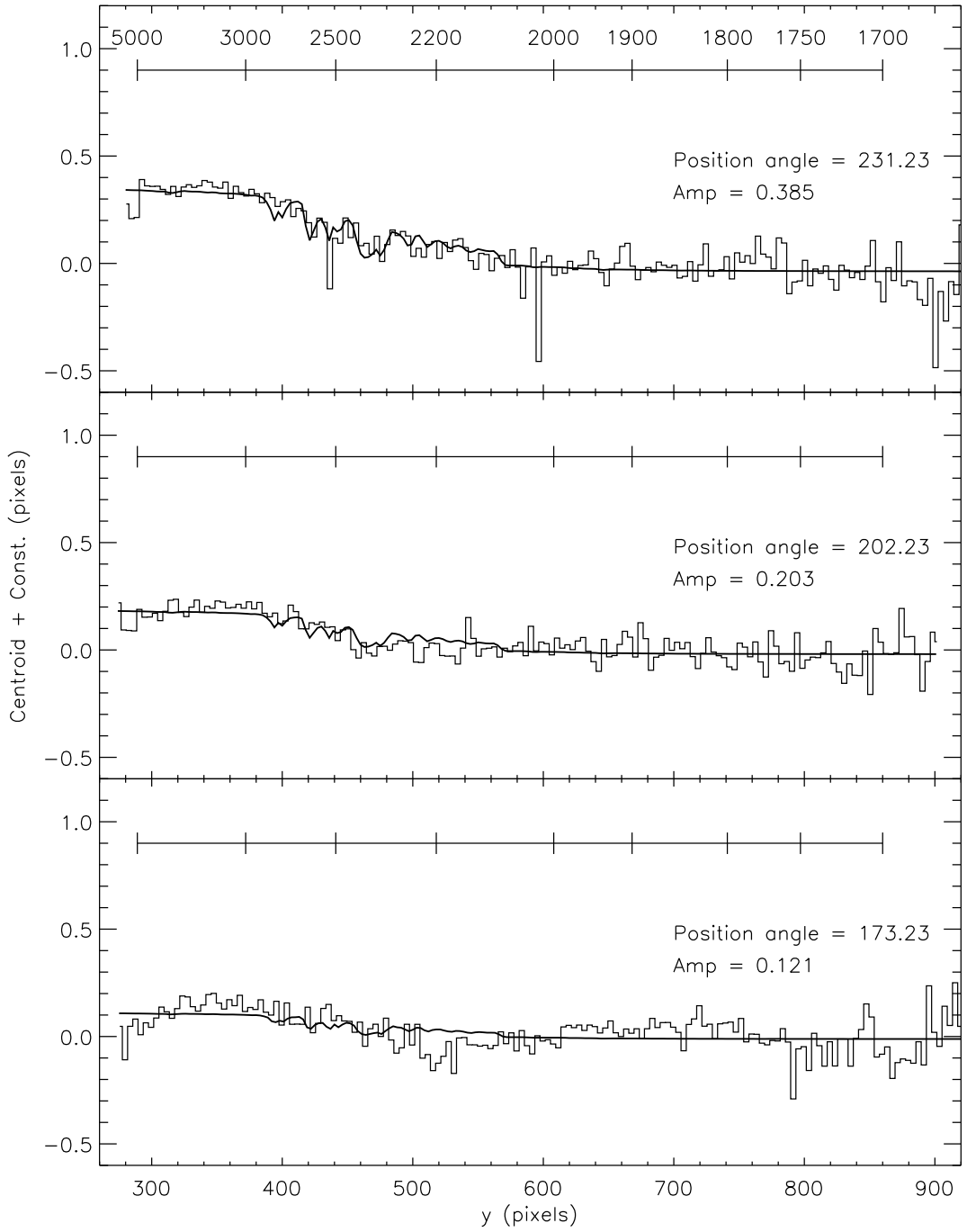

Fits to the mean centroids at each roll angle for U Aql. Each mean centroid was fit with a combination of $[1 + R(\lambda)]^{-1}$ determined from Kurucz models passed through an FOC spectra and a fourth order polynomial to represent the residual distortions. The curves shown have had the polynomial contributions removed. The models used to represent the binary were $T_{eff} = 5750$K and $\log g = 2.0$ for the primary and $T_{eff} = 10,000$K and $\log g = 4.0$ for the secondary, with $\Delta V = 4.25$ mag.

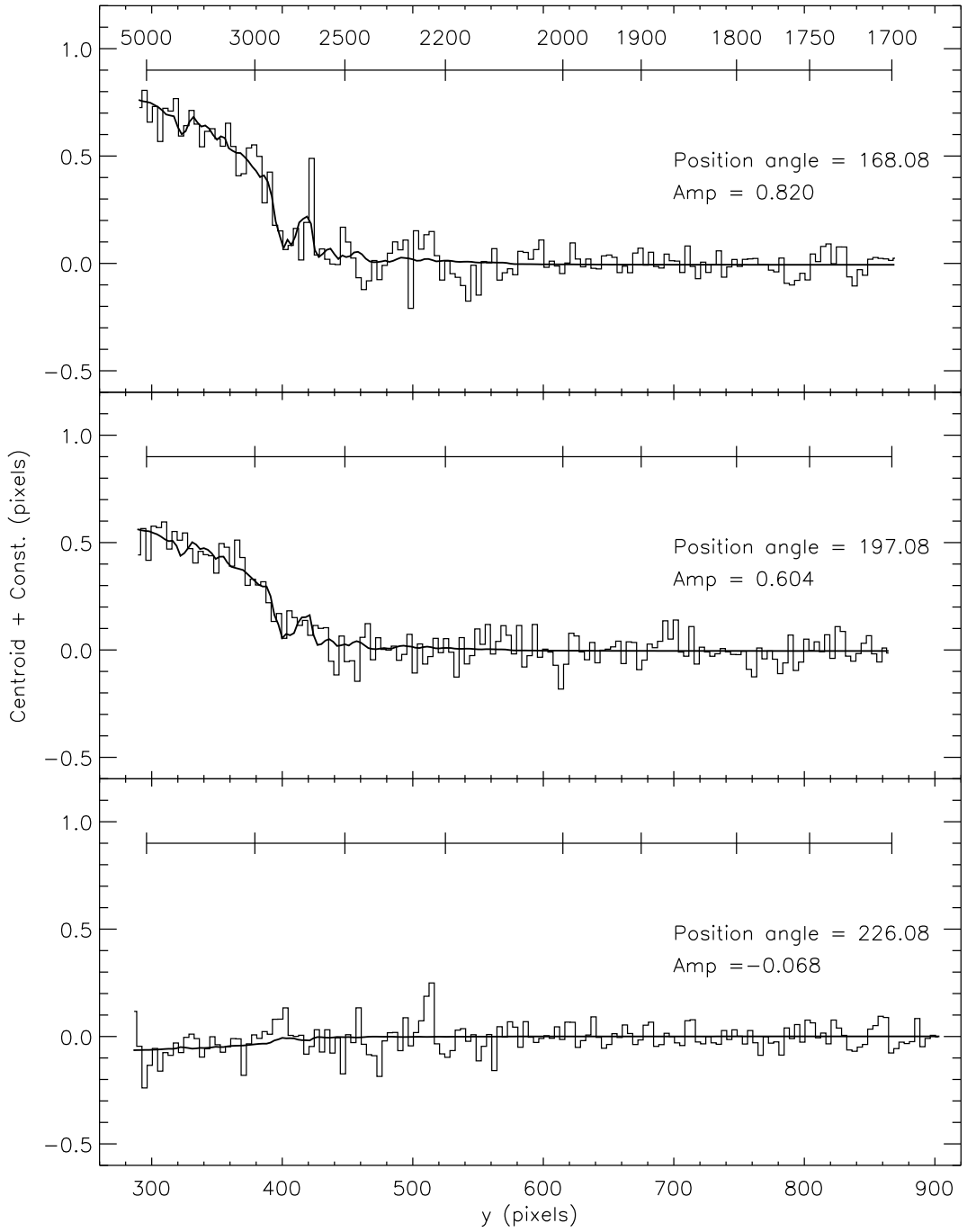

Fits to the mean centroids at each roll angle for AW Per. Each mean centroid was fit with a combination of $[1 + R(\lambda)]^{-1}$ determined from Kurucz models passed through an FOC spectra and a fourth order polynomial to represent the residual distortions. The curves shown have had the polynomial contributions removed. The models used to represent the binary were $T_{eff} = 5750$K and $\log g = 2.0$ for the primary and $T_{eff} = 11,500$K and $\log g = 3.5$ for the secondary, with $\Delta V = 2.5$ mag (Evans 1994).

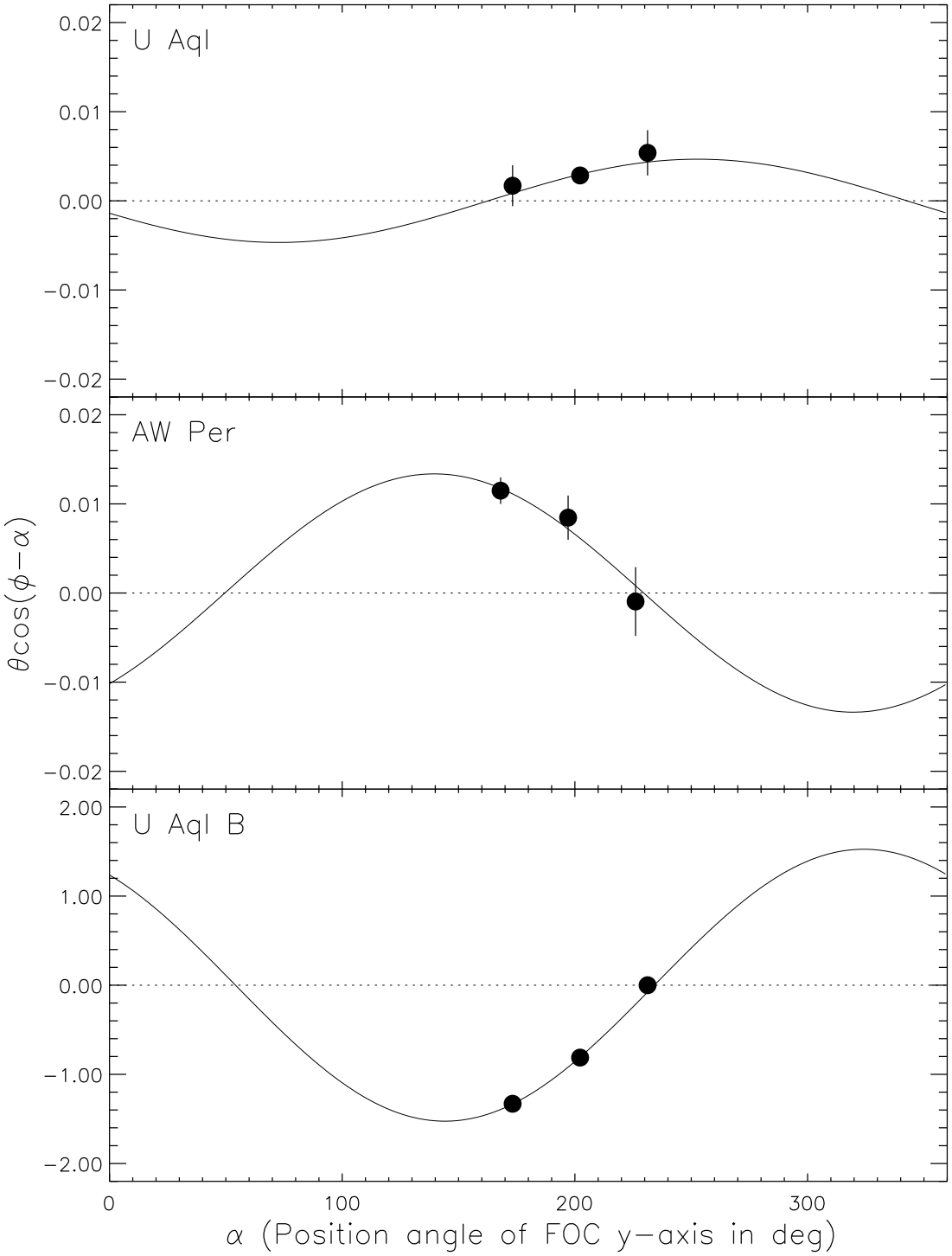

Determination of the angular separations and position angles of the program binaries. The observational errors were determined from individual fits to the 3 independent offset observations at each roll position.

Results for AW Per

- Angular separation
  $\theta = 0.013 \pm 0.003''$.
- Position angle
  $\alpha = 310 \pm 13^\circ$

Future

- FOC will be decomissioned soon, so there will be no second set of FOC observations to determine $\sin i$ for AW Per.
- Although STIS MAMA's have lower spatial resolution and poorer single detector wavelength coverage, they do have:

Geometrically distinct pixels	$\Rightarrow$	actual errors will be less since the FOC systematics dominated.
Better photometric sensitivity	$\Rightarrow$	same integration times provide more accurate results ($\sigma(x) \propto \alpha/\sqrt{N}$).
Better spectral resolution	$\Rightarrow$	can use the spectral features in $x(\lambda)$ to determine Δx.
Accurate absolute flux calibration	$\Rightarrow$	can fit the spectrum to obtain a more reliable $R(\lambda)$.

- Thus, it may be possible to obtain better accuracy with STIS in spite of its shortcomings for our application.
- Observations are scheduled to begin in June.